

Supporting Information

Realizing Deep-Ultraviolet Second Harmonic Generation by First-Principles-Guided Materials Exploration in Hydroxyborates

Pifu Gong,[†] Lei Kang,^{†,} and Zheshuai Lin^{†,‡,*}*

[†] Technical Institute of Physics and Chemistry, Chinese Academy of Sciences, Beijing 100190, China

[‡] Center of Materials Science and Optoelectronics Engineering, University of Chinese Academy of Sciences, Beijing 100049, China

List of Contents

Figure S1. Exploration map for achieving balanced NLO performance from $\text{KB}_5\text{O}_{12}\text{H}_8$ and $\text{CaB}_3\text{O}_6\text{H}$ to $\text{Sr}_2\text{B}_{11}\text{O}_{22}\text{H}_7$, $\text{SrB}_8\text{O}_{15}\text{H}_4$ and $\text{CaB}_8\text{O}_{15}\text{H}_4$.

Figure S2. $\text{B}_8\text{O}_{11}(\text{OH})_4$ (a), 2D $(\text{B}_8\text{O}_{11}(\text{OH})_4)_\infty$ layers (b) and crystal structure of $\text{SrB}_8\text{O}_{15}\text{H}_4$ (c).

Figure S3. Experimental powder XRD of $\text{CaB}_8\text{O}_{15}\text{H}_4$ (a) and $\text{SrB}_8\text{O}_{15}\text{H}_4$ (b).

Figure S4. Band structures, PDOS and SHG density plots of $\text{CaB}_8\text{O}_{15}\text{H}_4$ (a) and $\text{SrB}_8\text{O}_{15}\text{H}_4$ (b).

Table S1. Experimental and calculated crystallographic data of $\text{CaB}_8\text{O}_{15}\text{H}_4$ and $\text{SrB}_8\text{O}_{15}\text{H}_4$.

Table S2. Sellmeier equations of $\text{CaB}_8\text{O}_{15}\text{H}_4$ and $\text{SrB}_8\text{O}_{15}\text{H}_4$.

Table S3. NLO properties of typical DUV NLO borates, fluorooxoborates and hydroxyborates.

Table S4. Calculated mechanical properties of $\text{CaB}_8\text{O}_{15}\text{H}_4$ and $\text{SrB}_8\text{O}_{15}\text{H}_4$ as compared with KBBF.

Figure S1. Exploration map for achieving balanced NLO performance from $\text{KB}_5\text{O}_{12}\text{H}_8$ and $\text{CaB}_3\text{O}_6\text{H}$ to $\text{Sr}_2\text{B}_{11}\text{O}_{22}\text{H}_7$, $\text{SrB}_8\text{O}_{15}\text{H}_4$ (SBOH) and $\text{CaB}_8\text{O}_{15}\text{H}_4$ (CBOH).

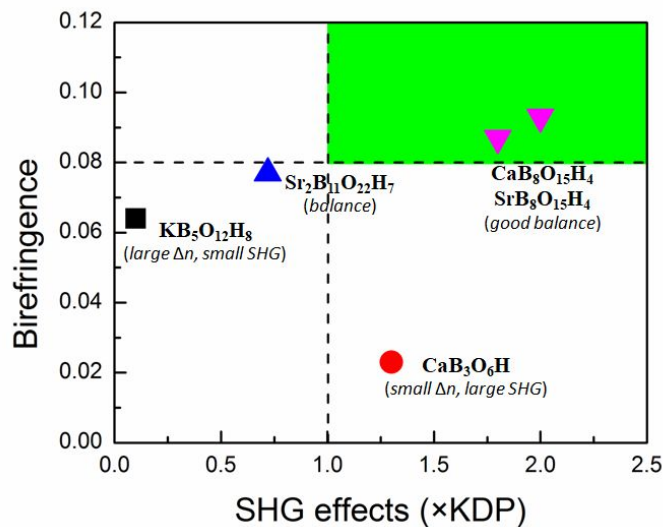


Figure S2. $[B_8O_{11}(OH)_4]$ (a), 2D $[B_8O_{11}(OH)_4]^\infty$ layers (b), and crystal structure of SBOH (c).

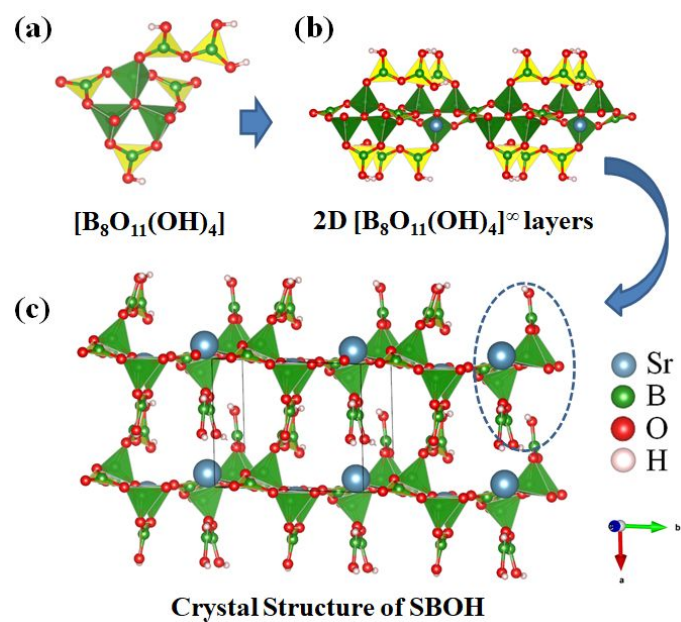


Figure S3. Experimental powder XRD of CBOH (a) and SBOH (b).

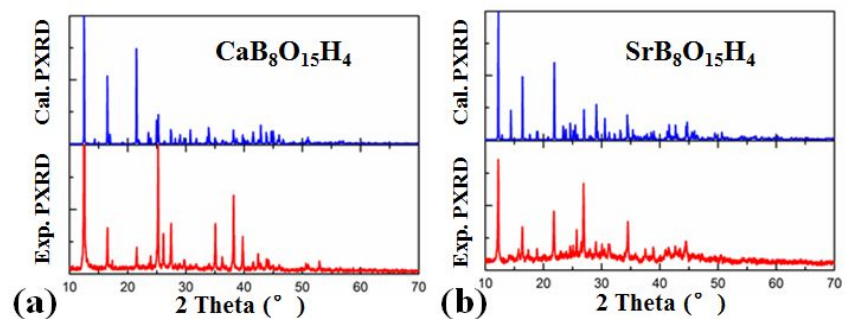


Figure S4. Band structures, PDOS and SHG density plots of CBOH (a) and SBOH (b).

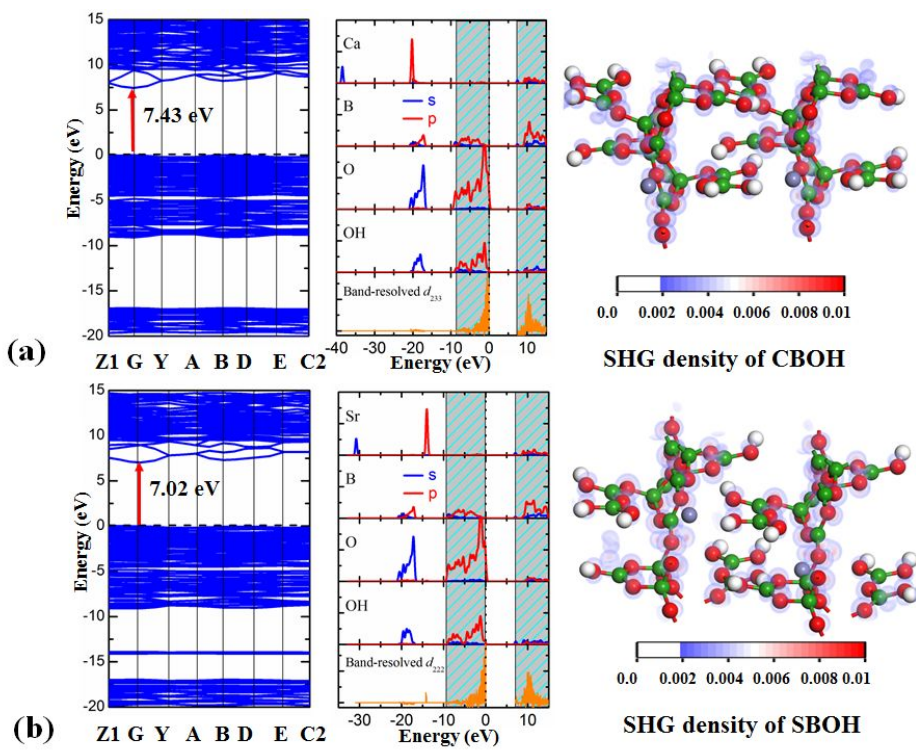


Table S1. Experimental and calculated crystallographic data of CBOH and SBOH.

Symmetry			<i>a</i> (Å)	<i>b</i> (Å)	<i>c</i> (Å)	β (°)	ICSD No.
CBOH	P2 ₁	Exp.	7.481	8.269	9.859	108.76	171019
		Cal.	7.508	8.195	9.546	107.88	
		Error	0.4%	-0.9%	-3.2%	-0.8%	
SBOH	P2 ₁	Exp.	9.909	8.130	7.623	108.40	4228
		Cal.	9.672	8.151	7.763	109.59	
		Error	-2.4%	0.3%	1.8%	1.1%	

Table S2. Sellmeier equations of CBOH and SBOH.

Sellmeier equations	
CBOH	$n_x^2 = 2.174422 + \frac{0.007486}{\lambda^2 - 0.012107} - 0.004989 \times \lambda^2$
	$n_y^2 = 2.094756 + \frac{0.006701}{\lambda^2 - 0.010771} - 0.002815 \times \lambda^2$
	$n_z^2 = 2.358048 + \frac{0.009303}{\lambda^2 - 0.011491} - 0.003896 \times \lambda^2$
SBOH	$n_x^2 = 2.386125 + \frac{0.009413}{\lambda^2 - 0.012677} - 0.006278 \times \lambda^2$
	$n_y^2 = 2.137378 + \frac{0.006950}{\lambda^2 - 0.012009} - 0.004888 \times \lambda^2$
	$n_z^2 = 2.206868 + \frac{0.007753}{\lambda^2 - 0.012633} - 0.003995 \times \lambda^2$

Table S3. NLO properties for typical DUV NLO borates, fluorooxoborates and hydroxyborates.

Compounds	Shortest PM wavelength (nm)	SHG Intensity (\times KDP)
γ -Be ₂ BO ₃ F (γ -BBF)	146	2.3
NaBe ₂ BO ₃ F ₂ (NBBF)	185	1.3
KBe ₂ BO ₃ F ₂ (KBBF)	161	1.3
RbBe ₂ BO ₃ F ₂ (RBBF)	174	1.3
CsBe ₂ BO ₃ F ₂ (CBBF)	202	1.3
NH ₄ Be ₂ BO ₃ F ₂ (ABBF)	174	1.17
NH ₄ B ₄ O ₆ F (ABF)	158	3.0
Ca ₂ B ₁₀ O ₁₄ F ₆ (CBOF)	171	2.3
Sr ₂ B ₁₀ O ₁₄ F ₆ SBOF)	169	2.5
NaB ₄ O ₆ F (NBF)	166	0.9
RbB ₄ O ₆ F (RBF)	165	0.8
CsB ₄ O ₆ F (CBF)	172	1.9
CsKB ₈ O ₁₂ F ₂ (CKBF)	170	1.9
CaB ₈ O ₁₅ H ₄ (CBOH)	174	2.0
SrB ₈ O ₁₅ H ₄ (SBOH)	185	1.8

Table S4. Calculated mechanical properties of CBOH and SBOH as compared with KBBF.

	Bulk Modulus (GPa)	Young Modulus (GPa)		
		x	y	z
KBBF	42 (exp. 44) ^a	228	228	39
CBOH	42	58	81	114
SBOH	34	115	46	48

^a Ref. Jiang, X. X.; Luo, S. Y.; Kang, L.; Gong, P. F.; Yao, W. J.; Huang, H. W.; Li, W.; Huang, R. J.; Wang, W.; Li, Y. C.; Li, X. D.; Wu, X.; Lu, P. X.; Li, L. F.; Chen, C. T.; Lin, Z. S. Isotropic Negative Area Compressibility over Large Pressure Range in Potassium Beryllium Fluoroborate and its Potential Applications in Deep Ultraviolet Region. *Adv. Mater.* **2015**, 27, 4851-4857.